Experimental confirmation of the von Neumann theory of shock wave reflection transition

By FILIPE J. BARBOSA† AND BERIC W. SKEWS

School of Mechanical Engineering, University of the Witwatersrand, Private Bag 3,
WITS 2050, South Africa

For many years there has been debate regarding why shock wave reflection off a solid surface has allowed regular reflection to persist beyond the incidence angles where it becomes theoretically impossible. Theory predicts that at some limiting angle the reflection point will move away from the wall and Mach reflection will occur. Previous studies have suggested that the paradox could be due to the presence of the growing viscous boundary layer immediately behind the point of reflection, and some numerical studies support this view. This paper takes the approach of establishing an experimental facility in which the theoretical assumptions regarding the surface of reflection are met, i.e. that the reflecting surface is perfectly smooth, perfectly rigid, and adiabatic. This is done by constructing a bifurcated shock tube facility in which a shock wave is split into two plane waves that are then allowed to reflect off each other at the trailing edge of wedge. The plane of symmetry between the waves then acts as the perfect reflection surface.

Through a careful set of visualization experiments, and the use of multivariate analysis to take account of the uncertainty in shock Mach number, triple-point trajectory angle, and slightly different shock wave arrival times at the trailing edge, the current work shows that the transition from one type of reflection to the other does indeed occur at the theoretical value. Conventional tests of reflection off a solid wall show significantly different transition results. Furthermore, it is also shown that the thermal boundary layer plays an important role in this regard. It is thus confirmed that viscous and thermal effects are the reason for the paradox. Reasons are also suggested for the counter-intuitive behaviour of the reflected shock wave angle.

---

1. Introduction

The transition of shock wave reflection geometry from a regular to a Mach reflection pattern was first described analytically by von Neumann (1943) and has been the subject of significant research ever since. In regular reflection the incident shock wave (I) and the reflected shock wave (R) meet at the surface of reflection at a point known as the reflection point, as shown in figure 1(*a*). Depending on (M_s, γ, θ_w) space, where M_s, γ and θ_w are the incident shock wave Mach number, gas specific heat ratio and flow deflection angle respectively, ten different reflection geometries have been observed, see Ben-Dor (1992). Holding M_s constant and reducing the flow deflection angle (θ_w), regular reflection transitions into a geometry known as single Mach reflection (henceforth referred to as Mach reflection). This transition results in significantly different pressure ratios behind the shock wave, which has implications

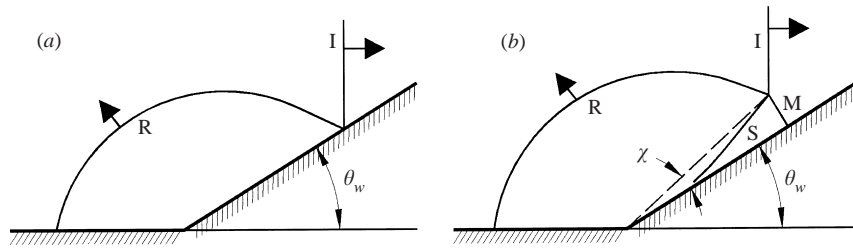† Present address: McKinsey & Co., P.O. Box 652767, Benmore 2010, South Africa.

FIGURE 1. Shock wave reflection geometries. (*a*) Regular reflection. (*b*) Mach reflection.

for aerodynamic and blast loading calculations. Figure 1(*b*) illustrates the Mach reflection geometry where the reflection point has detached from the surface and an additional shock wave, known as the Mach stem (M), now connects the incident and reflected shock waves to the surface. The intersection of the three shock waves is known as the triple point and the angle between the triple-point trajectory and the surface is known as the triple-point trajectory angle (χ). The slipstream (S) is a thermodynamic contact discontinuity which separates the gas that has passed through the incident and reflected shock waves from the gas that has passed through the Mach stem.

The basic equations that describe regular and Mach reflection, known as two- and three-shock theory respectively, were formulated by von Neumann (1943). The analysis applied the oblique shock wave equations to the regions in close proximity to the reflection or triple point, with relevant geometrical and boundary conditions. In the case of pseudo-steady flow a Galilean velocity transform is performed to make the reflection or triple point stationary. Thus the equations are strictly true only for the fluid streamline passing through the reflection or triple point. The basic assumptions of the theory are: that the fluid is inviscid, that all the waves are infinitely thin and plane (and separate areas of uniform fluid) and that in the case of pseudo-steady flow the geometry is self-similar and thus can be treated as steady using a Galilean velocity transform. Additionally the three-shock theory assumes that the triple-point trajectory is straight and emanates from the leading edge of the reflecting wedge.

Three transition criteria were proposed by von Neumann (1943) and are known as the sonic, detachment and mechanical equilibrium criteria. The detachment criterion predicts that transition occurs when the maximum flow deflection angle across the reflected shock wave is reached and a two-shock-wave solution is no longer possible. The sonic transition criterion suggests that transition occurs when the flow behind the reflected shock wave becomes sonic, allowing the corner signal, originating from the initial deflection, to be communicated to the reflection point. This transition mechanism was discussed by Bleakney & Taub (1949) and by Kawamura & Saito (1956) who both stated that for pseudo-steady flow conditions the sonic and detachment criteria were not experimentally distinguishable. Lock & Dewey (1989) were able to experimentally distinguish between the detachment and sonic criteria, and determined that transition occurred at the sonic point for their set of experiments. The mechanical equilibrium criterion (which requires a smooth pressure change during transition) has been observed to apply to some steady flows, but in the domain of low Mach number pseudo-steady flows in air, the mechanical equilibrium has no solution.

1.1. *The persistence of regular reflection*

Significant experimental research was performed on shock wave reflections during World War II, particularly at Princeton University. L. G. Smith (1945), at the sug-

gestion of von Neumann, performed a comprehensive set of shock tube experiments and produced quantitative data on wave angles and reflection geometries over a complete range of deflection angles for $1.04 < M_s < 3$. Three important conclusion were reached that have been confirmed by subsequent researchers:

(i) Prior to transition two-shock theory is in remarkable agreement with experimental observation.

(ii) For strong shock waves ($\approx M_s > 1.5$) three-shock theory shows reasonable agreement with experiments. However three-shock theory fails badly in the weak shock wave domain.

(iii) Persistence of regular reflection, well past the theoretical maximum limits, is consistently observed in experiments.

L. G. Smith (1945) suggested that a possible source of the discrepancy was the fact that the waves might be significantly curved in the region of the triple point and that the optical system used did not have sufficient resolution to confirm this. These inconsistencies in three-shock theory and the persistence of regular reflection have become known collectively as the 'von Neumann paradox'. Bleakney & Taub (1949) confirmed the observations by re-measuring the results of L. G. Smith (1945) and by performing additional experiments wherein transition was inferred, for a given M_s, by measuring the triple-point trajectory angle and extrapolating to zero. Bleakney & Taub (1949) raised the possibility that thermal and viscous effects caused the von Neumann paradox, but concluded that they probably did not play an important role, as borne out by the remarkable success of two-shock theory prior to transition. Bleakney & Taub (1949) stated that the probable cause of the discrepancies was the existence of variations in density in the domains bounded by the assumed planar waves, although they could not observe these in their experiments. The persistence of regular reflection implies, in the steady frame of analysis, that there exists flow into the wall and that the conservation laws are violated, and thus has been the focus of significant investigation.

1.2. *Reasons for the persistence of regular reflection*

The primary reason why viscous and thermal boundary layers were not considered as the cause for persistence of regular reflection was that the boundary layer displacement thickness was so thin, starting from zero behind the shock wave and building up to a few microns 1 mm later, under typical test conditions. In a seminal paper Hornung, Oertel & Sandeman (1979) confirmed that transition to irregular reflection in steady flows occurred at the mechanical equilibrium condition and that transition in pseudo-steady flows occurred at the sonic point. They proposed the length scale criterion as a mechanism that predicted the correct transition point in both steady and pseudo-steady flows. In addition they also suggested that viscous and thermal boundary layer phenomena were in fact the cause of the persistence of regular reflection and they put forward a physical mechanism by which this occurred. Their fundamental premise was that it was the shape of the boundary layer in the vicinity of the reflection point and not the height, as this is known to be extremely small, that is important. Hornung *et al.* (1979) noticed a viscous effect in the transition to irregular reflection in the results of Takayama & Sekiguchi (1977) on shock reflection over a cone. The difference between the observed shock wave inflow angle at transition (ϕ_{1tr}) and the theoretical maximum shock wave inflow angle (ϕ_{1d}), corresponding to the detachment condition, increased with a decrease in Reynolds number (Re) as the driver conditions were altered. Hornung *et al.* (1979) also observed that the persistence of regular reflection was absent or less pronounced in the internal cavity
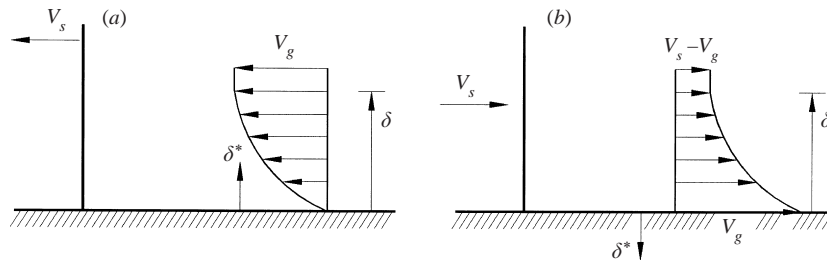
FIGURE 2. Boundary layer behind a shock wave: (*a*) laboratory frame;
(*b*) pseudo-steady frame.

experiments of W. R. Smith (1959) and of Henderson & Lozzi (1975). These internal cavity experiments were designed to reflect two plane waves into each other, their plane of symmetry being a perfect inviscid adiabatic boundary. Neither W. R. Smith nor Henderson & Lozzi associated the lack of regular reflection persistence with the elimination of the boundary layer at the reflection surface.

Hornung *et al.* (1979) explained the persistence of regular reflection due to the boundary layer on the reflecting surface as follows: Figure 2(*a*) illustrates the velocity profile of a boundary layer behind a moving shock wave. In order to apply the shock wave equations to this system a Galilean velocity transform is used to transform the system to a frame of reference wherein the shock wave is motionless. The shock wave and resulting boundary layer velocity distribution in this pseudo-steady frame of reference is illustrated in figure 2(*b*). It can be seen that in the pseudo-steady frame of analysis the shock tube wall now has a velocity V_s relative to the shock wave. This means that the wall velocity V_s is larger than the relative gas velocity $V_s - V_g$, resulting in a negative boundary layer displacement thickness δ^*, that acts as a mass sink. The pseudo-steady inviscid analogue of the above situation for regular reflection is illustrated in figure 3. The negative boundary layer displacement thickness in the viscous case results in a displaced wall in the inviscid analogue. This in turn results in an offset flow deflection angle ϵ, which relaxes the requirement for the reflected shock wave to turn the flow back parallel to the wall, and thus allows for the persistence of regular reflection past the inviscid theoretical maximum. Hornung *et al.* (1979) also proposed a future experiment whereby the Reynolds number be varied at a constant Mach number to allow the confirmation of this hypothesis. The only anomaly was that according to their physical reasoning it was expected that the angle between the reflected shock wave and the wedge (ω') would decrease; however the opposite was observed. No explanation for this was offered. This anomaly was not observed in subsequent work by Shirouzu & Glass (1982).

1.3. *The experiment of Hornung & Taylor* (*1982*)

Hornung & Taylor (1982) carried out shock wave reflection experiments, in a free-piston shock tube, at constant incident shock wave Mach number and velocity, i.e. constant temperature, while varying the initial shock tube pressure p_1. Thus Hornung & Taylor were able to perform a series of tests at $M_s = 5.5$ in argon (to avoid substantial real gas effects) and observe the transition from regular reflection to double Mach reflection at a variety of Reynolds numbers. For each series of tests the non-dimensionalized Mach stem height (linear analogue of χ) was plotted versus the inflow angle ϕ_1 (the angle between the incident shock wave and the approaching flow, in the pseudo-stationary frame of reference). A line was fitted through these data and
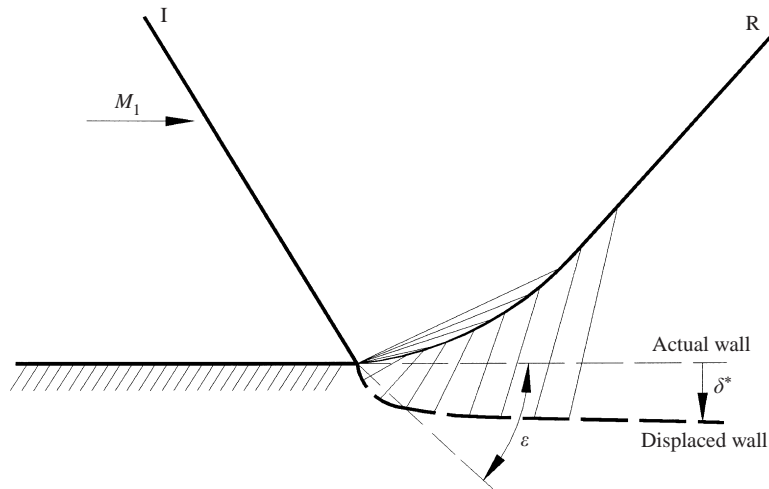
FIGURE 3. The negative displacement effect due to the boundary layer – inviscid analogue.

extrapolated to a zero value of the non-dimensionalized Mach stem height, to obtain the value of ϕ_1 at transition to regular reflection. Four series of tests were performed at different values of p_1 and thus at different Re. These points were extrapolated to obtain a value of ϕ_1 at transition for an infinite Re. This equated to a zero velocity boundary layer thickness (δ) (applicable to compressible boundary layer flow over a flat plate, see Anderson 1991),

$$\delta = \frac{5x}{\sqrt{Re}} fn\left(M_e, Pr, \frac{T_w}{T_e}\right), \qquad (1.1)$$

where the subscripts e and w refer to the free-stream and wall conditions respectively, x is a suitable length scale and M, T and Pr are the Mach number, temperature and Prandtl number. If the thermal conductivity (k), specific heat (C_p) and dynamic viscosity are assumed constant or solely a function of temperature (a perfect gas under reasonable conditions) then Pr is a function of temperature only and the boundary layer thickness varies only with Re, when M and T are held constant. Within Hornung & Taylor's experimental accuracy, their value of ϕ_1 was identical to that calculated using the sonic transition criteria, thus indicating that viscous effects were the cause of the persistence of regular reflection. Shirouzu & Glass (1982) re-checked existing experiments for viscous dependence and Wheeler (1986) performed additional experiments by scaling initial pressure. Both these studies illustrated that the reflection transition had a viscous dependence, but did not provide quantitative confirmation of the hypothesis of Hornung *et al.* (1979).

The work of Ben-Dor (1987) amongst others has illustrated the importance of viscosity in the region of the triple point and slipstream, and how it substantially affects the shock reflection geometry, see Ben-Dor (1992). The experiment of Hornung & Taylor (1982) did not isolate the viscous effects at the surface of reflection but rather inferred the effect of zero viscosity throughout the entire flow field. Assuming that the displacement effect of the shear layer that issues from the triple point behaves smoothly, then the extrapolation, performed by Hornung & Taylor (1982), determines the correct transition point.

It is well known that in the case of the compressible boundary layer behind a moving shock wave the walls of the shock tube (which are colder than the free gas, especially

in fairly strong shock waves) act as a mass sink (Thompson 1972, p. 507). Thus it can be expected that the thermal transport at the reflection wall can also contribute significantly to the persistence of regular reflection. This was experimentally validated by van Netten, Dewey & von Haimberger (1994) who, by heating and cooling the reflection surface, illustrated that thermal conduction significantly affects the reflection geometry. Subsequent numerical simulations by Henderson, Crutchfield & Virgona (1997, p. 32) confirmed this and proved that for certain flow conditions the thermal transport effect dominates the viscous transport mechanism in causing a significant delay in eruption of the self-similar nature of the shock reflection. Their numerical solutions of the Navier–Stokes equations with isothermal slip boundary conditions demonstrated that thermal effects strongly influence reflection transition even without the presence of a velocity boundary layer. It is thus instructive to consider both viscous and thermal effects in the experiments of Hornung & Taylor (1982). By extrapolating to infinite Re, Hornung & Taylor did in fact reduce the effect of the viscous boundary layer, while keeping all other variables constant. Since Pr is positive and near unity, in the limit, the effect of this extrapolation is to reduce the size of the thermal and viscous boundary layers to zero. However the gas in the experiment remained at a constant temperature and thus maintained a constant and finite viscosity and thermal conductivity throughout the extrapolation. One can thus expect that a finite heat transfer, from the hot gas behind the shock wave to the cool shock tube wall, still exists as Re approaches infinity. The results of Henderson *et al.* (1997) are thus understandable, but the relative contribution of the thermal effects as transition is approached, such as in the extrapolation process of Hornung & Taylor (1982), are still to be clarified.

The heat transfer from the gas to the shock tube wall can be characterized using the Nusselt number (Nu), which is the dimensionless temperature gradient at the wall surface. The relationship between the flow properties and Nu in a compressible boundary layer behind a moving shock wave is given by Schlichting (1968, pp. 422–426) as

$$Nu = \sqrt{Re_x}\, fn' \left(\frac{V_g}{V_s}, Pr \right) = \sqrt{Re_x}\, fn'' \left(\frac{M_g}{M_s}, Pr, \frac{T_2}{T_1} \right). \tag{1.2}$$

Here the subscripts 1, 2 refer to the gas properties ahead of and behind the shock wave respectively, while s and g refer to the shock wave and the gas behind the shock wave respectively. It can be seen that in the constant Mach number and constant temperature experiments, performed by Hornung & Taylor (1982), Nu was solely dependent on Re. As Re approached infinity so Nu also approached infinity. The relationship between Nu and the heat flux q is given by Schlichting (1968, p. 262) as

$$q = \frac{k}{l} Nu(T_w - T_e), \tag{1.3}$$

where l is an appropriate distance. Equation (1.3) shows that for constant temperature conditions (and thus constant k) the heat flux approaches infinity as Nu approaches infinity. Since persistence of regular reflection was not present in Hornung & Taylor's experiments, this suggests that these thermal effects do not significantly affect transition under their experimental conditions (i.e. thermal boundary layer thickness approaching zero).

1.4. *Other experiments*

W. R. Smith (1959) conducted a series of internal cavity experiments at $M_s = 1.04$, wherein a V-shaped test section was added to the end of a shock tube which was
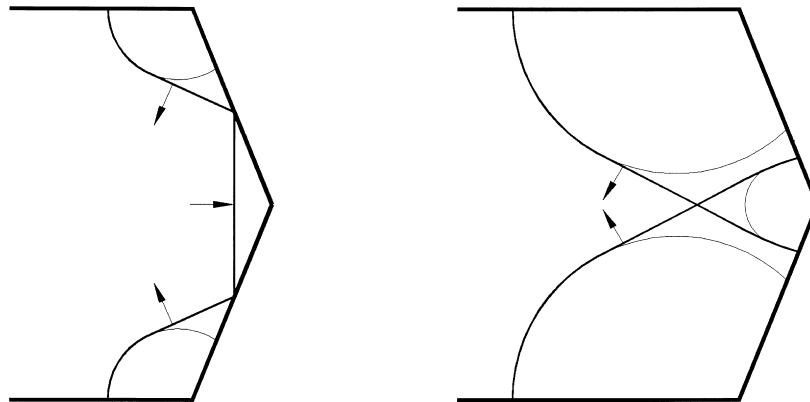
FIGURE 4. W. R. Smith's cavity experiment arrangement.

so angled as to reflect the planar incident wave towards the centre from both walls, see figure 4. Thus the two reflected waves reflect off each other at the centre of the test section, their plane of symmetry acting as an *ideal* adiabatic inviscid surface of reflection. W. R. Smith (1959) observed that transition from regular to irregular reflection occurred at approximately the detachment point. Smith did not attribute this to the absence of transport phenomena but to more precise optical determination of the reflection transition, due to the absence of a physical boundary in the vicinity of the reflection point. Smith based his observation of the lack of persistence of regular reflection by extrapolating measured values of χ to zero; however re-examination of his experimental results throws doubts on his conclusion that persistence of regular reflection did not occur. Smith's curve fit through his data did not represent a statistical best fit curve, but rather a combination of a straight line and an arc. A curve fit through all Smith's data with χ values of greater than 0.2 indicates a definite persistence of regular reflection of greater than $2°$ $(\phi_1 + \chi)$. The data points which led him to observe experimental transition at the theoretically determined point were all for χ values of the order of $0.1°$. Smith's data set in this range had significant experimental scatter, in some cases greater than 300%. In addition the interferograms of the mutual reflection of equal strength shocks published by Smith (1959, figure 4) were clearly non-symmetrical. Smith (1959) and subsequent researchers such as Henderson & Lozzi (1975) and Virgona (1993) experienced several problems in obtaining accurate measurements using the internal cavity apparatus. These difficulties can be summarized as follows:

It is difficult to measure the strength of the reflected shock waves accurately. In addition the interaction of the reflected shock wave with the wall boundary layer causes lambda-type shocks, which are very thick and make accurate measurements of wave angles near transition impossible, see Virgona (1993). Also the presence of corner signals, see figure 4(*b*), severely limits the length of test time for which the reflected waves are planar. This means that in many experiments the data are obtained from very small Mach stem reflections, and thus have large errors.

Skews (1995) suggested that if it was possible to generate two separate plane waves that reflected off each other at the trailing edge of a wedge, see figure 5, then their plane of symmetry would act as an *ideal*, inviscid adiabatic, reflecting surface. Skews achieved this by using a bifurcated shock tube, shown in figure 6, wherein a plane shock wave is split by a splitter into two plane waves which then travel down separate
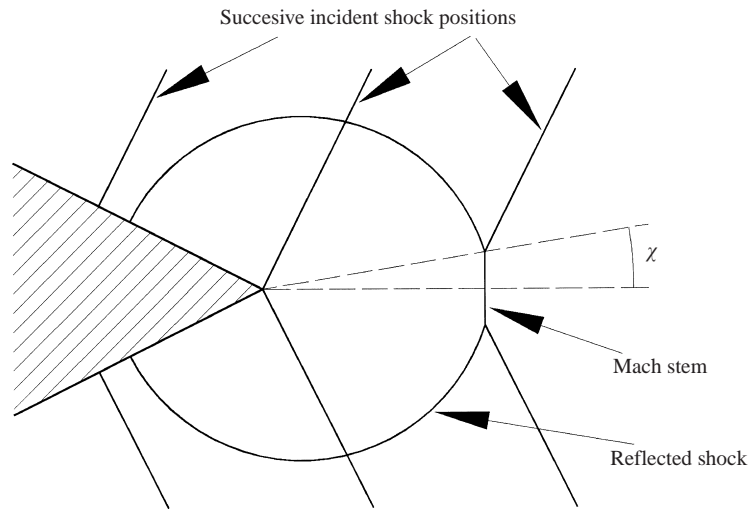
Succesive incident shock positions

FIGURE 5. Mutual reflection at the trailing edge of a wedge.

channels. These channels were bent in such a way as to bring the two shock waves together to interact at the trailing edge of a wedge. This bifurcated shock tube was able to generate synchronized shock waves in 20% of tests and indicated strongly that the persistence of regular reflection was indeed caused by transport mechanisms on the reflection surface, as hypothesized by Hornung *et al.* (1979). The purpose of this paper is to report on further bifurcated shock tube experiments, using a much larger facility that was able to produce high quality flow fields, that further tests the above hypothesis.

2. Experiment

2.1. *The bifurcated shock tube*

A series of experiments were performed in a bifurcated shock tube with a wedge angle of 80° (corresponding to a deflection angle of 40°). The test gas was air, with the driven gas being at ambient pressure and temperature. A double-diaphragm shock tube driver was used to generate a plane shock wave. The shock wave is split into two by the splitter which is a V-shaped machined channel with an angle of 80° between the two legs. The distance between the diaphragm and the splitter was 1.2 m (equivalent to 27 pipe diameters). Once the wave is split it enters a straight section followed by a long rolled section with an arc angle the same as that between the bifurcated legs. These sections were made from commercial tubing with internal dimensions of 44 mm high by 94 mm wide, rolled to a 3 m radius. The final straight section of the tube, which was 18 pipe diameters long, was accurately machined to match the test-section. The test-section, splitter and straightening sections were manufactured from mild steel blocks, using a numerically controlled milling machine, and the internal areas were polished smooth. Synchronization was adjusted by adding spacer sections to one of the curved legs. Due to the size of the shock tube (total length of 11 m) it was necessary to enclose the top and bottom curved legs within an enclosed loop made from insulated air-conditioning ducting. A small fan circulated the air within the duct to ensure that the ambient temperature was the same in both legs. Holographic interferograms showed that the bifurcated shock tube generated a
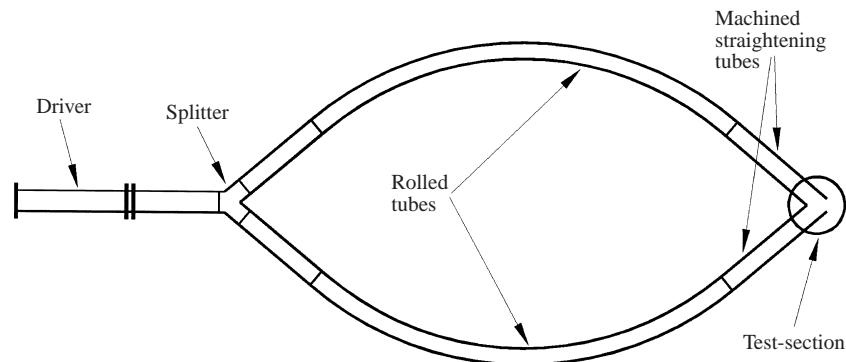
FIGURE 6. B. W. Skews' bifurcated shock tube geometry.

high quality uniform flow field. In all cases the difference in Mach number between the two incident shock waves was well below 0.2%.

2.2. *Flow visualization and measurement*

Contact shadowgraphs were obtained using a 30 ns pulsed ruby laser, aligned perpendicular to the test-section to within 0.05°. The images were recorded on 4 in. × 5 in. AGFA 10E75 holographic emulsion which was sandwiched against the rear test-section window. This emulsion has a resolution of 2800 lines/mm and was developed for 2 minutes using AGFA GP61 high-contrast developer. Contact shadowgraphs are very accurate since they have a magnification of unity and do not use any optics downstream of the test section. The shadowgraphs were scanned at 600 dots per inch using a high accuracy linear scanner with an error in aspect ratio of only 0.45%. This error was compensated for by stretching the images using bi-cubic resampling which stretches the image without degrading the quality. All scanned images were imported into a professional computer aided drawing package and measured electronically to an accuracy of 1 pixel. Sensitivity analyses were performed for each measurement, the results of which are given in the following section.

3. Results and discussion

Figures 7 and 8 show typical shadowgraphs obtained. The mis-synchronization between the two incident shock waves is given by δt which corresponds to the time difference between the arrival of the two shock waves at the wedge apex in the test-section. The corresponding mis-synchronization distance between the two waves is δx, i.e. the distance the early wave would be past the corner when the late wave is at the corner.

Tests with a mis-synchronization value of $\delta x \leqslant 1$ mm were assumed to be perfectly synchronized, since this value is the same order of magnitude as the visualized shock wave thickness. Table 1 is a summary of the experimental results for the synchronized tests. The angles ω_{ir} and ω_{rs} refer to the angle between the incident and reflected waves and the angle between the reflected wave and the slipstream respectively, while ΔM_s and $\Delta\chi$ are the maximum experimental uncertainties for M_s and χ. The angles ϕ_1, ω_{ir} and ω_{rs} have a uncertainty of approximately $\pm 1.6°$. These reflection angles are difficult to determine accurately since the reflected and Mach shocks and slipstream can possess substantial curvature in the vicinity of the triple point, and thus all measurements are constrained by optical resolution limits. These angles can
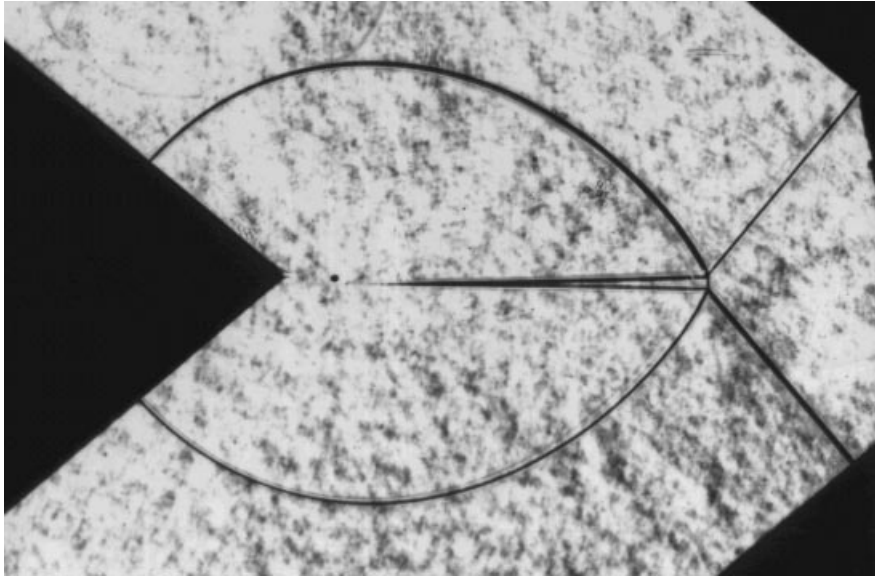
FIGURE 7. Shadowgraph for $M_s = 1.26$, $\delta t = 2.3\,\mu$s.

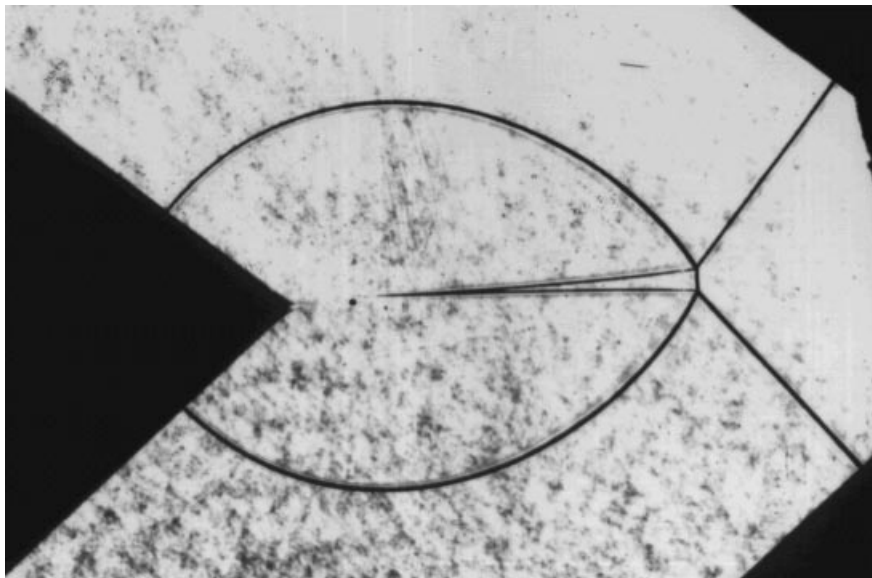FIGURE 8. Shadowgraph for $M_s = 1.33$, $\delta t = 1.4\,\mu$s.

be measured twice on each shadowgraph, due to the symmetry of the reflection, and thus the uncertainty was assumed to be equal to twice the average standard deviation of each reflection angle, throughout the series of synchronized tests.

3.1. *The extrapolated M_s versus χ curve*

Figure 9 shows the experimental M_s versus χ data along with a second-order least-squares curve fit through the data points. A second-order polynomial curve fit was found to be the most appropriate, producing an extremely accurate fit with a coefficient

M_s	ΔM_s	χ (deg.)	$\Delta\chi$ (deg.)	ϕ_1 (deg.)	ω_{ir} (deg.)	ω_{rs} (deg.)	δx (mm)
1.34	0.0030	1.64	0.07	50.3	71.0	61.7	0.05
1.33	0.0045	1.57	0.07	50.2	72.0	61.4	0.65
1.31	0.0035	1.39	0.06	50.3	71.6	61.2	0.22
1.26	0.0019	0.91	0.07	50.1	66.1	65.4	1.00
1.25	0.0032	0.85	0.07	50.1	65.5	65.2	0.03
1.20	0.0027	0.49	0.06	49.9	64.8	65.5	0.89
1.17	0.0020	0.20	0.12	50.2	–	–	0.94

TABLE 1. Synchronized (bifurcated shock tube) shock wave experiment results: $\theta_w = 40°$.
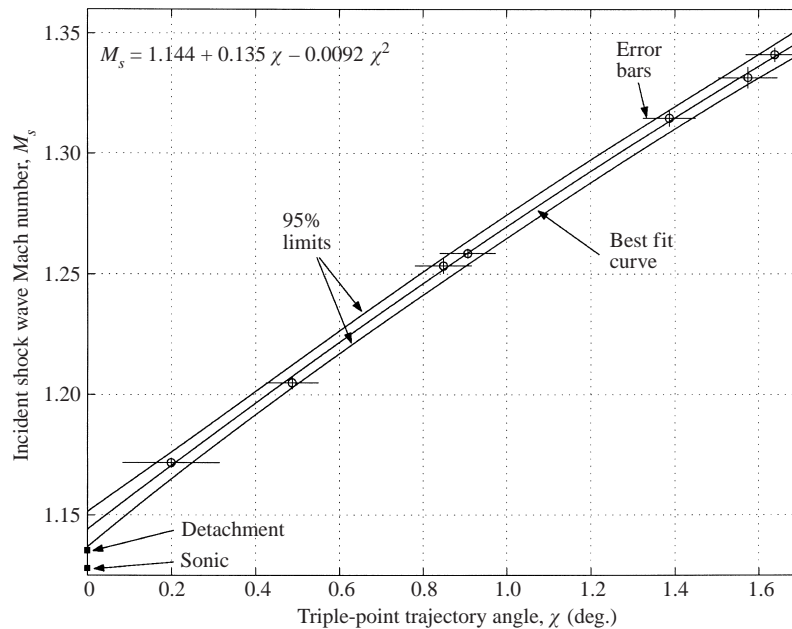
FIGURE 9. Experimental M_s versus χ curve, $\theta_w = 40°$: ——, quadratic best fit curve; $\bigcirc$, experimental points; +, error bars.

of determination of $r^2 = 99.93\%$ and M_s residuals of the order of 10^{-3}. Numerous researchers, such as Henderson *et al.* (1997), have also found that the triple-point trajectory angle curve can be modelled well by a second-order polynomial and that significant curvature does not occur as transition is approached. The detachment ($M_s = 1.135$) and sonic ($M_s = 1.128$) theoretical transition points as well as the 95% statistical confidence limits (which are a function of the standard deviation and the position of the extrapolated point from the mean of the experimental data and from the experimental points themselves) are also indicated on figure 9. The resulting extrapolation gives a value of $M_s = 1.144 \pm 0.007$ for the *ideal* transition point. This is essentially the same as the detachment point, within the experimental accuracy of $\Delta M_s = \pm 0.01$, thus indicating that the persistence of regular reflection is indeed due to transport effects on the surface of reflection. However within the extremely narrow 95% confidence limits the experimentally determined value is slightly larger than the theoretical transition values. A linear best fit line through the same data

M_s	χ (deg.)	ϕ_1 (deg.)	ω_{ir} (deg.)	ω_{rs} (deg.)
1.233	0.49	49.1	63.6	68.0
1.238	0.58	49.4	65.0	66.6
1.243	0.61	49.4	64.3	66.5
1.262	0.75	49.2	63.7	68.2
1.345	1.47	48.3	71.1	63.4
1.367	1.51	48.6	67.1	67.2
1.374	1.63	47.9	71.4	64.6
1.386	1.85	48.2	70.6	65.7
1.406	1.81	48.6	71.4	64.5
1.430	2.09	47.8	73.6	63.5
1.445	2.16	47.7	73.9	63.2

TABLE 2. Results of the 40° conventional wedge reflection tests.

produces essentially the same results (within 1%), but with the transition point being $M_s = 1.150 \pm 0.008$.

In order to compare this *ideal* reflection surface data with conventional wedge reflection tests a second series of tests in a conventional linear shock tube were performed. This shock tube has an automated double-diaphragm driver that is capable of generating high quality reproducible planar shock waves. A 40° wedge was manufactured out of mild steel and was polished to provide a smooth reflection surface. The wedge spanned the entire shock tube test section and the leading edge was raised substantially from the shock tube floor to eliminate any floor boundary layer effects. Contact shadowgraphs were again used to obtain the images; however a pulsed xenon white light source with a duration of about 1 µs was used. The images were recorded on standard 100 ASA emulsion. The results of these wedge reflection tests are given in table 2. A second-order polynomial was fitted through this data using least-squares regression and the transition Mach number was determined to be $M_s = 1.171 \pm 0.032$. Even with the large 95% confidence bounds the theoretical transition points still lie outside the predictions of this experiment, thus confirming the persistence of regular reflection in conventional wedge reflection tests as observed by all previous researchers.

3.2. *The effect of mis-synchronization: a multivariate analysis*

In order to be conclusive it is instructive to consider the effects of mis-synchronization (non-zero δx) on the bifurcated shock tube (*ideal* surface) experiments. Figure 7 illustrates the test which had the worst synchronization ($\delta x = 1$ mm) in the series of 'synchronized' tests. A very small circular vortex can be observed just downstream of the wedge apex. The two slipstreams emanating from the two triple points both terminate in this circular vortex. A small asymmetry can be observed due to the mis-synchronization.

Figure 10 is an exaggerated illustration of the shock wave interaction process in the case of mis-synchronized incident shock waves. The initial interaction is shown in figure 10(*a*) and can be explained as follows: The upper shock wave arrives first and sheds a vortex as it diffracts around the wedge apex. The later arriving lower shock wave undergoes an extremely weak shock–vortex interaction (which deforms the shock wave in the region of the vortex) and then relaxes back into a planar shock wave, see Ellzey *et al.* (1995). At point (1) the two shock waves, which are now of equal strength, interact for the first time as two planar shock waves reflecting off each
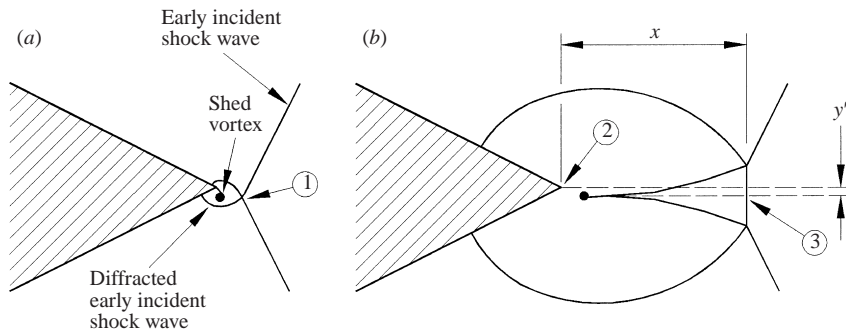
FIGURE 10. An exaggerated schematic of the mis-synchronized case. (*a*) Initial interaction. (*b*) Interaction at a later stage.

other. The conventional Mach reflection geometry evolves from this point onwards. Figure 10(*b*) shows the interaction process at a later time. It can be seen that almost the same reflection process has been generated from the slightly mis-synchronized case as would have been generated from the ideal synchronized case. The one exception is that the Mach reflection pattern has been displaced slightly downwards by a distance y', which would be expected to generate a form of parallax error in the measurement of χ angle data.

The triple-point trajectory angle is determined by calculating the arc-tangent of the Mach stem half-height y, divided by x, the distance from the wedge apex (point (2) in figure 10*b*) to the midpoint of the Mach stem (point (3)). In the perfectly synchronized case, point (2) is the correct location of the initial shock wave reflection. However in the slightly mis-synchronized case point (1) (figure 10*a*) is the correct location of the initial shock wave interaction point. Thus in the mis-synchronized case, x will always be measured as slightly larger than its real value and the angle χ will be consistently larger than the value calculated. Thus it would be expected (if only perfectly synchronized tests were obtained) that the M_s versus χ curve (figure 9) would shift to the right causing the transition Mach number to be lower than that which was determined. This means that the true value would be even closer to the theoretical transition Mach number than that which was obtained. The logical measurement of relative mis-synchronization is the non-dimensional value $\delta x/x$. Here δx is the mis-synchronized distance between the two incident shocks, as previously defined. This non-dimensional value is multiplied by a factor of 100, to obtain a percentage mis-synchronization, and will be referred to as ψ.

Table 3 lists the M_s, χ and ψ values for the seven synchronized tests and for a further six slightly mis-synchronized ($\psi \leqslant 20$) tests. A nonlinear least-squares multivariate regression analysis was performed and it was found that a two-dimensional quadratic function between M_s, χ and ψ best approximated these 13 data points. The resulting three-dimensional surface is specified by

$$M_s = 1.135 + 0.143\chi - 0.011\chi^2 + 0.0014\psi + 0.00007\psi^2. \qquad (3.1)$$

Once again the resulting regression fit is extremely accurate, with all M_s residuals being smaller than 0.005. To obtain the transition value at perfect synchronization both χ and ψ are set to zero in (3.1); additionally the 95% confidence limits were calculated as before, resulting in a transition value of $M_s = 1.135 \pm 0.01$, which is identical to the theoretical detachment transition point. The theoretical sonic transition point is also well within the confidence bounds. A linear (three-dimensional plane) regression fit

M_s	χ (deg.)	ψ
1.17	0.20	4.44
1.20	0.49	2.24
1.25	0.85	0.09
1.26	0.91	2.72
1.26	0.93	3.14
1.31	1.24	8.09
1.31	1.29	6.63
1.31	1.39	0.55
1.33	1.57	1.81
1.34	1.52	4.24
1.34	1.64	0.14
1.35	1.28	17.50
1.35	1.31	16.10

TABLE 3. Results of all bifurcated shock tube tests with $\psi \leqslant 20$.

through these data produces essentially the same result with less than a 1% difference in transition which is predicted to occur at $M_s = 1.139 \pm 0.01$.

Figure 11 is a comparison between the conventional wedge reflection tests and the results of the multivariate analysis (equation (3.1)) on the bifurcated shock tube data. This figure unambiguously shows that the hypothesis of Hornung *et al.* (1979), that persistence of regular reflection is solely due to transport effects at the surface of reflection, is in fact true. It must be re-emphasized that the regression fit through the bifurcated shock tube data in figure 11 is actually a three-dimensional curve with the value of ψ set to zero (perfect synchronization) and with the ψ-axis suppressed. In addition, although the data points that were assumed to be synchronized ($\delta x \leqslant 1$ mm) are superimposed on the plot, they are not the only data points that were used in the respective regression analyses. The full range of data points given in table 3 were used to perform the regression analyses. It is instructive to note the effect of the test at $M_s = 1.17$ on the regressed curve: the measured value of χ for this test case was 0.2° which is significantly smaller than the next smallest χ value of 0.49°. As a consequence of the small value of χ this test has very large horizontal error bars as can be seen in figure 9. The question arises of the veracity of using a point with such large uncertainty. It is possible that this point could artificially induce the curvature in the regressed polynomial to force it to attain the theoretical transition value. To verify whether this does indeed occur another multivariate regression analysis was performed with this point left out of the data set. The result of this analysis, that transition occurs at $M_s = 1.131 \pm 0.025$, is essentially the same as the previous case. This experimental transition point lies exactly in between the theoretical transition points determined using the detachment and sonic criteria, with both points lying well inside the 95% confidence limits again. This confirms the fact that the three-dimensional quadratic function models the experimental data extremely accurately and that there is no large change in curvature rate as χ approaches zero.

3.3. *Comparison of reflection angles with theoretical predictions*

As observed by Hornung & Taylor (1982), and in contradiction to the findings of Shirouzu & Glass (1982), the angle between the reflected shock wave and the surface of reflection (ω') was larger in the viscous case than in the inviscid case, which was contrary to what is expected from the physical arguments of Hornung & Taylor
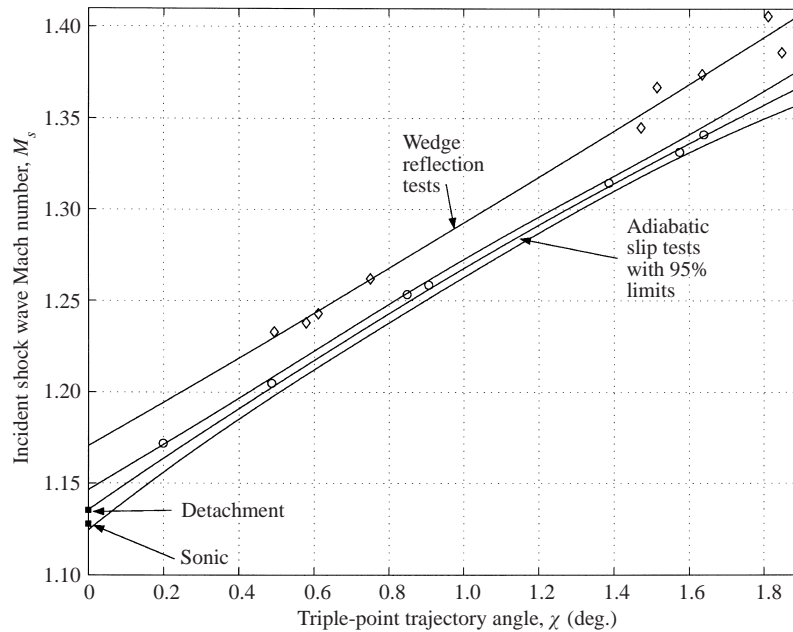
FIGURE 11. Comparison between conventional wedge tests ($\Diamond$) and the bifurcated shock tube (adiabatic, slip) experimental M_s versus χ and ψ surface: $\psi = 0$ and ψ-axis suppressed, $\theta_w = 40°$: ——, quadratic best fit curve (at $\psi = 0$) with 95% confidence bounds; $\bigcirc$, assumed synchronized experimental points ($\delta x \leqslant 1$ mm) – remaining 6 data points not shown.

(1982) since in the viscous case the reflected shock wave does not have to deflect the flow as much, due to the negative displacement effect of the boundary layer. The difference in ω' is approximately $2°$ and increases slightly with M_s. Comparisons of the reflection angles χ, ω_{rs} and ω_{ir} obtained in the conventional wedge reflection tests and the bifurcated tests with theoretical predictions are shown in figures 12, 13 and 14. The theoretical predictions shown are those obtained using three-shock theory, modified three-shock theory (values of χ prescribed using experimental values, and the requirement that the flow on either side of the slipstream is parallel relaxed) and the theory proposed by Sandeman (2000). The modified three-shock theory is seen to be inaccurate in all cases and breaks down at $M_s \approx 1.3$, when ϕ_2 reaches $90°$ and the pressures across the slipstream are no longer matched. Although Sandeman's theoretical predictions are more accurate than three-shock theory, in most instances, significant deviations from theory still exist for some reflection angles when compared to the bifurcated shock tube experiments. Thus the broader 'von Neumann paradox' (especially at weak Mach numbers) still exists.

3.4. *Possible physical causes of discrepancies*

Although the bifurcated shock tube results prove conclusively that persistence of regular reflection is solely due to transport effects on the reflection surface, figures 13 and 14 show that the removal of the viscous and thermal boundary layer on the wedge surface actually increases the wave angle discrepancies between von Neumann three-shock theory and experiment. This clearly indicates that the overall influence of transport properties on the reflection process is more complex than outlined in the arguments put forward by Hornung *et al.* (1979). The angles ω' and ω_{ir} behave in a counter-intuitive way: for a set incident shock strength and flow deflection (wedge)
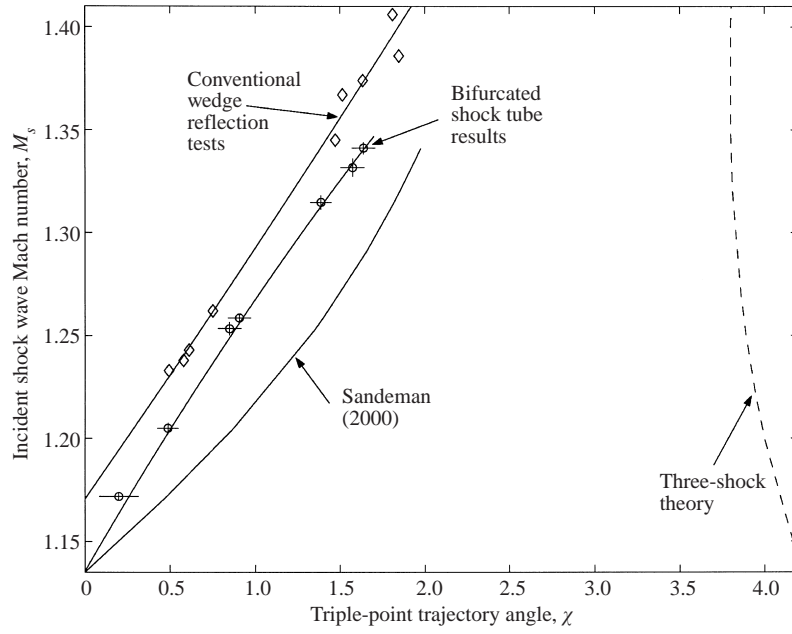
FIGURE 12. Theoretical and experimental M_s versus χ curves. $\theta_w = 40°$: ○, bifurcated tube data points; ◇, wedge reflection tests; +, error bars.

FIGURE 13. Theoretical and experimental ω_{rs} versus M_s curves. $\theta_w = 40°$: ○, bifurcated tube data points; ◇, wedge reflection tests; +, error bars.
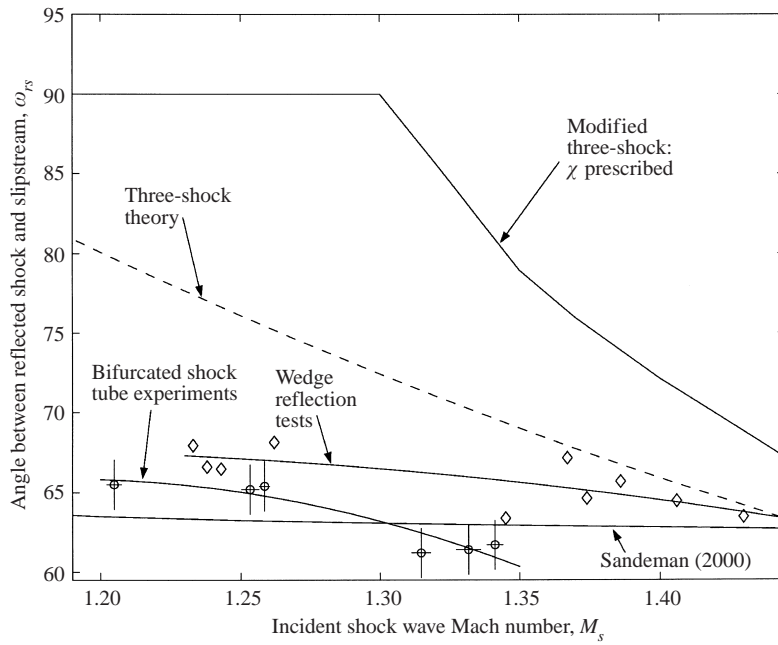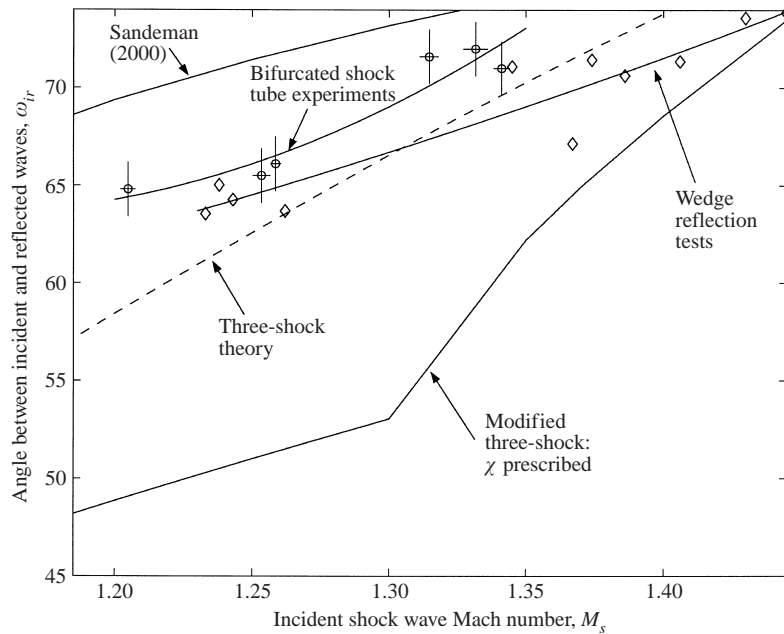
FIGURE 14. Theoretical and experimental ω_{ir} versus M_s curves. $\theta_w = 40°$: $\bigcirc$, bifurcated tube data points; $\diamondsuit$, wedge reflection tests; $+$, error bars.

angle the orientation and the strength of the incident shock wave is fixed and thus ϕ_1, the shock inflow angle (see figure 15), is constant. The incident shock wave flow deflection angle θ_1 is thus also a constant and can be calculated using the oblique shock relations. In an inviscid calculation the orientation and strength of the regular reflection is determined by the boundary condition that the flow must be turned back parallel to the wedge. The reflected shock wave obtained is always observed to be of the weak branch of the shock deflection polar and thus the relationship between the shock inflow angle (ϕ_2) and the shock flow deflection angle (θ_2) across the reflected wave is in positive proportion, John (1984). This means that as ϕ_2 increases so does θ_2 and vice versa. For the case of a viscous wedge the negative boundary layer displacement argument (Hornung *et al.* 1979) predicts that the effective angle of the surface of reflection is increased directly behind the point of reflection. This results in a lowering of the reflected shock wave flow deflection angle θ_2. This decrease in θ_2 must be accompanied by a resultant decrease in the reflected shock wave inflow angle ϕ_2, since this shock lies on the weak branch of the shock deflection polar. To accommodate this decrease in ϕ_2 the reflected shock must rotate about the reflection point anti-clockwise. Thus it would be expected that the angle between the incident and reflected shock wave ω_{ir} would be larger in the wedge experiments (viscous) than in the bifurcated experiments (adiabatic slip). The opposite is observed as can be seen in figure 14.

It must be remembered that the bifurcated shock tube experiments are in gas of finite viscosity and thermal conductivity and that it is only along the surface of reflection that these effects are unimportant since there are no velocity and temperature gradients there. It is thus necessary to consider the influence that the slipstream (S), see figure 15, has on the overall reflection geometry. Ben-Dor (1987) considered the effects of finite viscosity on the slipstream and determined that these
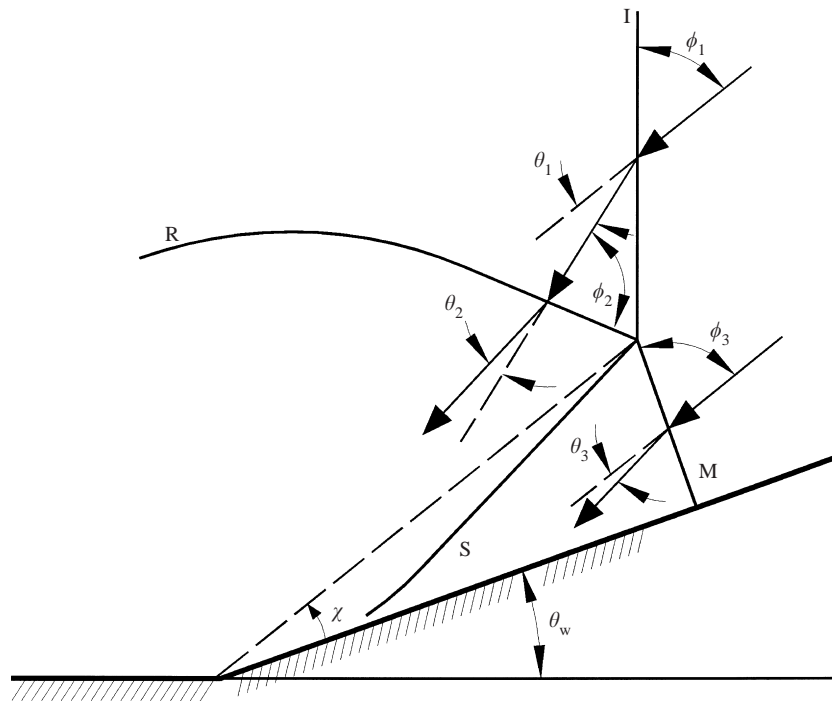
FIGURE 15. Schematic of Mach reflection – three-shock notation.

effects were in fact of major significance in altering the reflection angles. The flow velocity behind the reflected wave is higher than that behind the Mach stem, thus a momentum exchange occurs between these two regions.

Considering the effect of the adiabatic slip reflection surface boundary condition on a typical Mach reflection system (figure 15) one is able to obtain some pointers as to how this boundary condition can influence the orientation of the reflected shock wave. Dewey & McMillin (1985) showed that viscosity on the wedge surface prevents the Mach stem from being perpendicular to the wedge. However in the bifurcated tube experiments the Mach stem has to be perpendicular to the wedge since the flow in front of the Mach stem is initially parallel to the reflection surface and it must remain so in the absence of transport effects along the wedge. The Mach stem cannot however remain perfectly straight throughout its length since the deflection of the streamline that passes through the triple point is non-zero. Although the Mach stem is not seen to be curved, it must possess a gentle curvature as it approaches the triple point. Thus the boundary condition along the wedge affects the curvature of, and the resultant flow behind, the Mach stem. The gas velocity, in the region between the slipstream and the reflected shock wave (in the domain of these experiments) and in the triangular region bounded by the wedge, the slipstream and the Mach stem, is subsonic relative to the triple point. Thus a disturbance in either of these two regions is always communicated to the triple point. Additionally the gas in these two regions is strongly coupled by the thermal energy and momentum interchange across the slipstream – which increases on moving away from the triple point as the slipstream thickens (this can even eventually break down into a vortex street).

Using these simple physical arguments it is easy to see how changes in the wall boundary condition can dramatically affect the size, shape and flow properties of

the triangular patch behind the Mach stem. This in turn alters the orientation and properties of the slipstream which in turn has been shown by Ben-Dor (1987) to strongly affect the reflection wave angles surrounding the triple point. This explanation in terms of Mach reflection geometry shows that the effects of wedge boundary conditions are more complex and coupled than the simplified regular reflection arguments of Hornung *et al.* (1979). This outcome is natural since the flow discussed in Hornung *et al.*'s experiment was a globally inviscid one, while the bifurcated shock tube flow is much more complex with strong viscosity and thermal effects along the slipstream but none of these effects along the reflecting surface.

4. Conclusion

The bifurcated shock tube experiments have successfully provided further conclusive proof that the persistence of regular reflection is solely due to transport phenomena at the surface of reflection. The behaviour of the wave angles ω_{ir}, ω_{rs} and ω' is counter-intuitive and although a plausible physical explanation has been suggested, a full understanding of this phenomena would require high resolution Navier–Stokes numerical simulations. None of the three theoretical models used are totally successful in the weak Mach reflection domain of this experiment.

REFERENCES

ANDERSON, J. D. 1991 *Fundamentals of Aerodynamics*, 2nd edn. McGraw-Hill.

BEN-DOR, G. 1987 A reconsideration of the three-shock theory for a pseudo-steady Mach reflection. *J. Fluid Mech.* **181**, 467–484.

BEN-DOR, G. 1992 *Shock Wave Reflection Phenomena*, pp. 1–164. Springer.

BLEAKNEY, W. & TAUB, A. H. 1949 Interaction of shock waves. *Rev. Mod. Phys.* **21**, 584–605.

DEWEY, J. M. & MCMILLIN, D. J. 1985 Observation and analysis of the Mach reflection of weak uniform plane shock waves. Part 1. Observations. *J. Fluid Mech.* **152**, 49–66.

ELLZEY, J. L., HENNEKE, M. R., PICONE, J. M. & ORAN, E. S. 1995 The interaction of a shock with a vortex: Shock distortion and the production of acoustic waves. *Phys. Fluids* **7**, 172–184.

HENDERSON, L. F., CRUTCHFIELD, W. Y. & VIRGONA, R. J. 1997 The effects of thermal conductivity and viscosity of argon on shock waves diffracting over rigid ramps. *J. Fluid Mech.* **331**, 1–36.

HENDERSON, L. F. & LOZZI, A. 1975 Experiments on transition of Mach reflexion. *J. Fluid Mech.* **68**, 139–155.

HORNUNG, H. G., OERTEL, H. & SANDEMAN R. J. 1979 Transition to Mach reflexion of shock waves in steady and pseudosteady flow with and without relaxation. *J. Fluid Mech.* **90**, 541–560.

HORNUNG, H. G. & TAYLOR, J. R. 1982 The transition from regular to Mach reflection of shock waves Part 1. The effect of viscosity in the pseudosteady case. *J. Fluid Mech.* **123**, 143–153.

JOHN, J. E. A. 1984 *Gas Dynamics*, 2nd edn. Allyn & Bacon, Inc. Boston.

KAWAMURA, R. & SAITO, H. 1956 Reflection of shock waves – 1 Pseudo-stationary case. *J. Phys. Soc. Japan* **11**, 584–592.

LOCK, G. D. & DEWEY, J. M. 1989 An experimental investigation of the sonic criterion for transition from regular to Mach reflection of weak shock waves. *Exps. Fluids* **7**, 289–292.

VAN NETTEN, A. A., DEWEY, J. M. & VON HAIMBERGER, T. 1994 The effects of surface temperature on the shock wave reflection process. *Proc. 11th Mach Reflection Symposium, Victoria, Canada* (ed. J. M. Dewey). University of Victoria.

VON NEUMANN, J. 1943 Oblique reflection of shocks. *Bur. Ord. Explosives Res. Rep.* 12.

SANDEMAN, R. J. 2000 A simple physical theory of weak Mach reflection over plane surfaces. *Shock Waves* **10**, 103–112.

SCHLICHTING, H. 1968 *Boundary-Layer Theory*, 6th edn. McGraw-Hill.

SHIROUZU, M. & GLASS, I. I. 1982 An assessment of recent results on pseudo-stationary oblique-shock-wave reflections. *UTIAS Rep.* 264.

SKEWS, B. W. 1995 Synchronized shock tubes for wave reflection studies. *Rev. Sci. Instrum.* **66**, 3327–3330.

SMITH, L. G. 1945 Photographic investigation of the reflection of plane shocks in air. *OSRD Rep.* 6271.

SMITH, W. R. 1959 Mutual reflection of two shock waves of arbitrary strengths. *Phys. Fluids* **2**, 533–541.

TAKAYAMA, K. & SEKIGUCHI, H. 1977 An experiment on shock diffraction by cones. *Rep. Inst. High Speed Mech., Tohoku Univ., Sendai, Japan* **36**, 53–74.

THOMPSON, P. A. 1972 *Compressible-Fluid Dynamics*. McGraw-Hill.

VIRGONA, R. J. 1993 A study of shock wave diffraction from regular to irregular reflection and the effects of gas viscosity. PhD thesis, Dept. Mech. Engng., University of Sydney.

WHEELER, J. 1986 An interferometric investigation of the regular to Mach reflection transition in pseudostationary flow in air. *UTIAS Techn. Note* 256.